Proceedings of the EuroGNC 2013, 2nd CEAS Specialist Conference
on Guidance, Navigation & Control, Delft University of Technology,
Delft, The Netherlands, April 10-12, 2013

Detection of abnormal aircraft control surface positions using a robust parametric test

A. Gheorghe[1 2 3], A. Zolghadri[1], J. Cieslak[1], D. Henry[1]
P. Goupil[2], R. Dayre[2], H. Le Berre[2]

Abstract – For upcoming and future aircraft, one important challenge to tackle is the structural design optimization as it contributes to weight saving, which in turn helps improve aircraft performances (e.g. fuel consumption, noise, range) and consequently to decrease its environmental footprint. Jamming and runaway of a control surface could lead to significant structural loads and consequently must be considered in the aircraft structural design. A runaway is an untimely (or uncontrolled) deflection of a control surface which can go until its stops if it remains undetected. A jamming is a control surface stuck at its current position. In this paper, a procedure for robust and early detection of such failures is presented and it is shown that it significantly contributes to the aforementioned challenges. Firstly, an appropriate parametric model of the control servo-loop is estimated, and secondly, a fault is detected by means of a suitable decision test in the parametric space. It is shown that a particular parametric direction can be identified which is sensitive to the occurrence of the investigated faults. The proposed approach satisfies technical requirements in terms of false alarm, detection time and computational burden for real implementation. Experimental results with in-flight recorded data sets provided by Airbus are presented to show the efficiency of the proposed technique.

Nomenclature

FCC = Flight Control Computer
CR2 = Two confidence region
RARX = Recursive Autoregressive Model with Exogenous Input
FBY = Fly-by-Wire
FDD = Fault Detection and Diagnosis
RLS = Recursive least squares
ARX = Autoregressive Exogenous Input

---

[1] *Univ. Bordeaux, IMS lab, 351 cours de la Libération, F-33400 Talence, France*
{anca.gheorghe; ali.zolghadri; jerome.cieslak; david.henry}@ims-bordeaux.fr
[2] *EYCC Flight Control System, Airbus Operations S.A.S., Toulouse, France*
{philippe.goupil; remy.dayre; herve.le-berre}@airbus.com
[3] *corresponding author*

1 Introduction and problem setting

Consider a typical Airbus structure of servo-loop control of aircraft moving surfaces (Fig. 1.1), where COM is the command channel and MON is the monitoring channel in the Flight Control Computer (FCC) [9]. The COM channel provides the main functions allocated to the computer (flight control law computation and the servo-control of moving surfaces). The MON channel ensures (mainly) the permanent real-time monitoring of the COM channel and of all the components of the flight control system (sensors, actuators, other computers, probes, etc). Each channel receives a dedicated control surface or actuator position thanks to dedicated sensors.

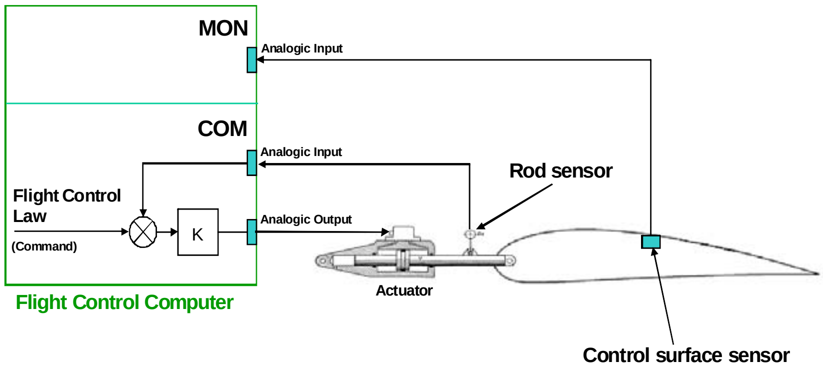

Figure 1.1 : Simplified block diagram of control surface servo-loop

This work deals with the faults located in the servo-loop of the moving surfaces, between the FCC and the control surface, including these two elements. It is assumed that faults impact only one control surface. Two fault cases are considered: runaway and jamming (Fig. 1.2). A runaway, or hard-over, is an untimely (or uncontrolled) control surface deflection, having very different dynamic behaviors, which can go until moving surface stops if it remains undetected [8, 9]. Runaway can have various speeds and are mainly due to electronic component failure, mechanical breakage or FCC malfunctions. A detected runaway will result in servo-control deactivation or computer passivation. After fault detection, the system is reconfigured and there is a hand-over between redundant computers and associated actuators in case of several actuators per control surface. A jamming (or lock in place failure) is a generic system-failure case which generates mechanical control surface stuck at its current position. A well-known negative effect of surface jamming is the resulting increased drag, which leads to increased fuel consumption. For example during a coordinated turn, if an elevator is jammed, the reaction of the aircraft is weaker and for compensating, more deflection will be demanded on the remaining elevator as well as on the Trimmable Horizontal Stabilizer. Due to the coupling with the roll axis, an additional dissymmetrical deflection of the aileron will be required. In case of landing with strong crosswind, the stuck rudder could generate additional drag. The two considered fault cases also lead to additional loads on the aircraft structure, correlated to the amplitude of the failure and must be taken into account in the structural system design.

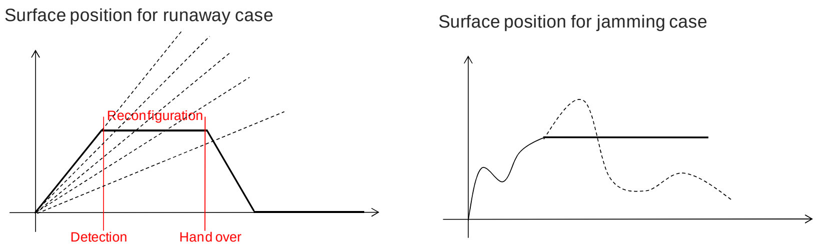

Figure 1.2 : Control surface position during runaway and jamming cases

The conventional techniques currently in use in aerospace systems ensure highest level of safety imposed by current certification process, provide sufficient fault coverage (all expected failures are anticipated and uncovered) and achieve a good robustness without false alarm [9, 16]. The current industrial practices for control surface runaway and jamming detection consist mainly in consistency checks between two redundant signals computed in the two FCC channels. If the difference between both signals is greater than a given threshold during a given time, the detection is confirmed. In the case of runaway, when the system reconfiguration is triggered, the control surface has reached a given position (deflection measured in degrees), which depends on the fault dynamic. The expected benefit of this work is a smaller control surface deflection when the runaway is detected and control surface jamming detection at lowest amplitudes. Consequently, the improvement of the current state-of-practice monitoring techniques is a challenging issue, as earlier runaway detection and reduction of the minimal detectable control surface jamming position, while keeping a good level of robustness, mean less loads generated on the aircraft structure, thus weight saving and reduced fuel consumption. From loads point of view, aircraft certification is obtained when it is proven that the structure complies with the dedicated regulations [17].

This work presents a parametric test for early detection of such failures, leading to early system reconfiguration, and to avoid significant unwanted structural loads. Other model-based control surface fault detection solutions, which preserve the structure of current and certificated detection techniques, are presented in [1, 2, 5].

The paper is organized as follows: a modified exponential forgetting algorithm for control surface servo-loop parameter estimation is formulated in section 2. Control surface servo-loop modeling is also presented in this section. A parametric test decision for on-line detection of abrupt changes is described in section 3. Section 4 is devoted to some simulation results based on real flight data. Finally, in section 5 some concluding remarks are given.

2 An exponential forgetting algorithm for control surface servo-loop parameter estimation

The problem of fault detection is formulated as a control surface servo-loop parameter estimation combined with a decision test in the parametric space. The parameters are estimated via recursive least-squares (RLS) algorithm with exponential forgetting modified for proper on-line implementation. We adopt black-box modeling obtained by system identification process [6]. In the open literature, many studies can be found for FDD using parametric models. See, among others, [10, 11, 12, 13, 14]. Here, it is shown that one of the estimated parameters is an indicator of the control surface runaway or jamming occurrence.

2.1 Parameter estimation method

The first step of the proposed solution consists in recursive parameter estimation of the above control surface servo-loop single-input (the commanded control surface deflection computed by the FCC according to the pilot order) single-output (the control surface position) dynamic system (Fig. 1.1). Black-box modeling offers the advantage to use the method for different systems, i.e. for different actuator models, different moving surfaces or different aircraft families.

Using all available measurements up to the current time, the input-output process dynamics can be described by the Recursive Autoregressive Model with Exogenous Input (RARX), written in a linear regression form:

$$y(k) = \varphi^T(k)\theta(k-1) + \varepsilon(k) \tag{1}$$

where k denotes the sampling index, $y(k)$ is the output to be predicted and $\varepsilon(k)$ is a term describing the noise effect on the system output. $\varphi(k)$ contains input and output measurements available at time k and $\theta(k)$ represents the unknown time-varying parametric model :

$$\begin{cases} \varphi^T(k) = [-y(k-1).....-y(k-na), u(k-nk)...u(k-nk-nb+1)] \\ \theta(k) = [a_1(k)....a_{na}(k), b_1(k)....b_{nb}(k)] \end{cases} \tag{2}$$

where na and nb are the order model structure and nk is the time delay between the input $u(k)$ and the output $y(k)$.

The estimated $\hat{\theta}$ of the unknown time-varying parameters θ is obtained by minimizing the loss function:

$$J = \sum_{i=1}^{k} \lambda^{k-i} (y(i) - \hat{y}(i))^2 \tag{3}$$

where λ is the forgetting factor, $\hat{\theta}$ is known as least squares (LS) estimate of θ and $\hat{y}$ is the predicted value of the output :

$$\hat{y}(k) = \varphi^T(k)\hat{\theta}(k-1) \tag{4}$$

Model (4) assumes that the predicted control surface position is a linear combination of past pilot order and control surface position measurements. A comparison between equations (1) and (4) shows that unknown parameter are estimated by minimizing the prediction error $\varepsilon(k)$.

The exponential forgetting algorithm consists of:

$$\begin{cases} \hat{\theta}(k) = \hat{\theta}(k-1) + K(k)\varepsilon(k) \\ \varepsilon(k) = y(k) - \varphi^T(k)\hat{\theta}(k-1) \\ K(k) = \dfrac{P(k-1)\varphi(k)}{\lambda + \varphi^T(k)P(k-1)\varphi(k)} \\ P(k) = \dfrac{P(k-1) - K(k)\varphi^T(k)P(k-1)}{\lambda} \end{cases} \tag{5}$$

where $P(k)$ is the covariance matrix and $K(k)$ is the innovation gain.

The choice of λ is a trade-off between fast adaptation and long term quality of the estimates. With a small value of the forgetting factor the estimated parameters converge to their true value quickly but the sensitivity to noise is increased. Typical choices of λ are in the range between 0.95 and 0.999 [6]. For robust on-line implementation in the FCC, some modifications of (5) are made. Care must be taken to prevent covariance wind-up. In fact, exponential forgetting is a method to discount older samples of data equally in all directions, so the most recent receive the greatest weighting. The approach works well if the incoming information is uniformly distributed both in time and in space. Especially for the control surfaces, when the major excitation comes from the variations of the command signal, this is seldom the case. Therefore, when the input is not persistent and the old data is discarded in the estimation procedure, the covariance matrix can grow exponentially and the estimation algorithm can stop before the parameters convergence.

One method to deal with wind-up is the well-known directional forgetting [14]. This algorithm is able to track fast parameter changes and is similar in complexity to the standard LS algorithm. The main difference with the classical LS method is how the covariance matrix and the innovative gain are updated. Contrary to the standard algorithm where old data are uniformly discarded and replaced by new data, for the directional forgetting, the covariance matrix and gain are updated only in the direction where new excited information is obtained. System (5) becomes:

$$\begin{cases} \hat{\theta}(k) = \hat{\theta}(k-1) + K(k)\varepsilon(k) \\ \varepsilon(k) = y(k) - \varphi^T(k)\hat{\theta}(k-1) \\ K(k) = \dfrac{P(k-1)\varphi(k)}{1+\varphi^T(k)P(k-1)\varphi(k)} \\ P(k) = P(k-1) - \dfrac{P(k-1)\varphi(k)\varphi^T(k)P(k-1)}{(\beta(k))^{-1} + \varphi^T(k)P(k-1)\varphi(k)} \\ \beta(k) = \begin{cases} \lambda - \dfrac{1-\lambda}{\varphi^T(k)P(k-1)\varphi(k)} & if\ \varphi^T(k)P(k-1)\varphi(k) > 0 \\ 1 & if\ \varphi^T(k)P(k-1)\varphi(k) = 0 \end{cases} \end{cases} \tag{6}$$

To avoid numerical instability and estimated parameters deviation, one of the most efficient and low computational load method is the Bierman factorization [7]. The main advantage of the method is that it requires no square roots, which is often time consuming compared with other arithmetic operations. The U-D Bierman decomposition factorizes the covariance matrix $P(k)$ into a set of matrices as follows:

$$P(k) = U(k)D(k)U^T(k) \tag{7}$$

where $U(k)$ is a unit upper triangular matrix, i.e. an upper triangular matrix with a unity diagonal and $D(k)$ is a diagonal matrix. Instead of updating the P matrix, U and D can then be updated in order to ensure method stability, numerical accuracy and to guarantee non-negativity of the computed covariance matrix.

2.2 Control surface servo-loop modeling

Using past control surface position and pilot order measurements, control surface servo-loop dynamics can be described by model (1). The modeling and identification process makes use of physical knowledge of the servo-loop behavior for choosing the model structure. Because one of the industrial constraints is to develop a method with reasonable computational burden, a second order model structure is chosen:

$$\hat{y}(k) = b_1(k-1)u(k-nk) - a_1(k-1)y(k-1) \tag{8}$$

where a_1 and b_1 are the unknown time-varying parameters to estimate and the time delay nk between the control surface servo-loop input and output is chosen according to in-flight recorded data sets.

For fault detection, when a runaway or a jamming occurs, the measured surface position is not consistent with the commanded control surface deflection. In the predicted output equation (8), the measured control surface position receives then the greatest weighting and almost no weight is put on the pilot order. Thus, one of the estimated parameter converges towards zero. That means that the change of estimated value b_1 to zero is an indicator of the control surface runaway or jamming case. Consequently, a decision test in the parametric space and not in the output space is used. The test will be detailed in section 3.

For a second order model structure, the unit upper triangular matrix $U(k)$ and the diagonal matrix $D(k)$ are:

$$U(k) = \begin{bmatrix} 1 & u_1(k) \\ 0 & 1 \end{bmatrix} \tag{9}$$

$$D(k) = \begin{bmatrix} d_1(k) & 0 \\ 0 & d_2(k) \end{bmatrix} \tag{10}$$

According to (7), (9) and (10) and considering $P(k) = \begin{bmatrix} p_{11}(k) & p_{12}(k) \\ p_{21}(k) & p_{22}(k) \end{bmatrix}$, the covariance matrix terms can be written as:

$$
\begin{cases}
p_{11}(k) = d_1(k) + u_1{}^2(k) d_2(k) \\
p_{12}(k) = u_1(k) d_2(k) \\
p_{21}(k) = u_1(k) d_2(k) \\
p_{22}(k) = d_2(k)
\end{cases}
\tag{11}
$$

Final equations to implement in the FCC for control surface runaway and jamming detection are obtained according to (6), where the decomposition (11) is introduced in the expressions of the innovation gain and the covariance matrix.

3 Two confidence regions (CR2) parametric decision test

The second step of the proposed solution consists in a parametric decision test. The CR2 test, developed in [3, 4], appears to be well situated for this application. The test is used here to detect an abrupt change of the estimated parameter. The method does not call for any optimization procedure and so offers the advantage of low computational expenditure. For more details about the CR2 test, the interested reader can refer to [3, 4]. In [3], it is shown that while in mono-dimensional case the CR2 test is equivalent to the well-known Chi2 test, their generalization in multi-dimensional case leads to different mechanization equations. The CR2 test is based on the overlap between the confidence regions associated with two estimates: one on-line estimate obtained via a modified exponential forgetting algorithm and another estimate which is computed from *a priori* information only.

Let be:

$\hat{\theta}_2(k)$: on-line estimated parameter b_1

$\hat{\theta}_1$: *a priori* nominal value of b_1, performed off-line by using a classical identification method

$C_2(k)$: on-line estimated covariance matrix relative to b_1 ; at each step, $C_2(k)$ matches with $p_{22}(k)$ in (11)

C_1 : nominal covariance matrix relative to b_1

α : detection threshold

The estimate $\hat{\theta}_2$ reflects the on-line estimations, which indicate the actual control surface behaviour, with respect to the “fault” or “fault-free” hypothesis. The estimate $\hat{\theta}_1$ reflects only *a priori* information and assumes the fault-free hypothesis. We assume that under fault-free hypothesis and using an appropriate forgetting factor, estimated parameter variations are relatively weak. Therefore, an abrupt change of the behavior of the parameter estimated is associated with a control surface runaway or jamming occurrence. Nominal parameter and covariance matrix are estimated off-line using a real data set. The estimates and their associated covariance matrix define two confidence ellipsoids centered on $\hat{\theta}_1$ and $\hat{\theta}_2$ in the parametric space (Fig. 3.1). The two confidence regions reflect all expected system behaviour. The fault detection procedure is used to decide if the observed changes can be explained satisfactorily in terms of the effect of noise and/or model uncertainties. If not, then we may conclude that a control surface fault has occurred. Specifically, as long as the two confidence regions overlap, the true parameter vector may be in both regions and it is reasonable to conclude that no failures have occurred. If the two confidence regions do not overlap, the true parameter vector cannot be in both regions simultaneously and a failure is declared.

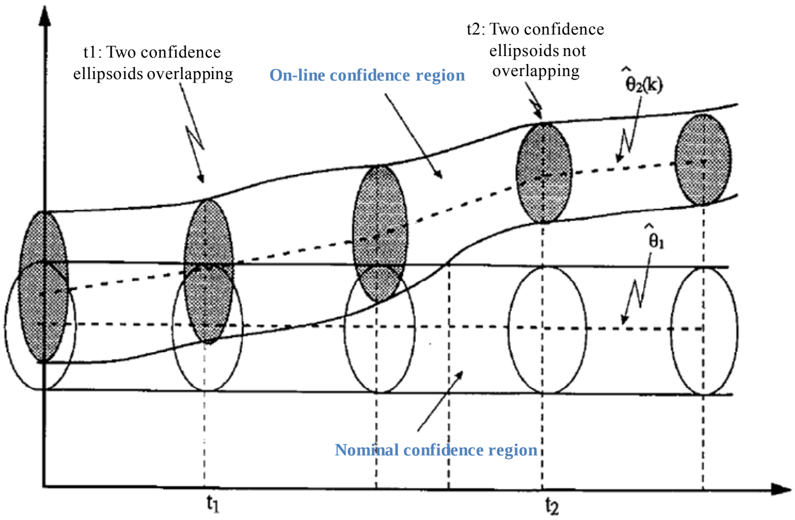

Figure 3.1 : Evolution of confidence regions when a fault occurs

The simplified mechanization equations (one-dimensional case) for the CR2 algorithm are summarized below (see [3] for the general case):

a) First verify that: $\dfrac{(\hat{\theta}_2(k)-\hat{\theta}_1)^2}{C_2(k)} > \alpha$.

If this inequality does not hold, the procedure stops (the confidence regions overlap).

b) Find with the dichotomy method (or using a 2nd order polynomial for one-dimensional particular case), the unique negative root λ_0 of F(λ), where :

$$F(\lambda) = \frac{V^2(\lambda)}{C_2(k)} - \alpha$$

$$V(\lambda) = \frac{C_2(k)(\hat{\theta}_2(k) - \hat{\theta}_1)}{\lambda C_1 - C_2(k)}$$

$F(-\infty) = -\alpha$ and $F(0) > 0$

with an initial value A<0 so that F(A)<0.

c) Consider the function: $W = \dfrac{C_1(\hat{\theta}_2(k) - \hat{\theta}_1)}{\lambda_0 C_1 - C_2(k)}$

$$test = \lambda_0^2 \frac{W^2}{C_1}$$

If $test > \alpha$ then the two confidence regions do not overlap and a fault is detected.

A test for the occurrence of a failure consists of comparing the overlap test to a constant threshold α. The threshold ensures the balance between detection delay and false alarm rate which are compliant with the structural design requirements and the operational constraints. A higher level of α to which the overlap test is compared, corresponds to larger confidence regions and so higher degree of robustness (low false alarm rate) with respect to unknown inputs such as uncertainties in the nominal model, system and measurement noise. However, an important threshold leads to a greater fault detection delay.

For Gaussian distributed prediction error $\theta - \hat{\theta}_1$ and $\theta - \hat{\theta}_2$, the threshold can be determined from tables of the Chi-squared distribution [15], depending on the confidence level, i.e. the probability that the true parameter vector lies within the confidence regions. In this work, the Chi-squared table is just used to establish an initial range of variations for α. The design parameter α is then chosen by injecting runaways and jammings on a real data set. With various thresholds within the operating range, different simulations are made in order to test the fault detection delay and the false alarm rate.

4 Experimental results

In order to check the robustness and the detection performances of the method, simulations are performed using a real data set recorded during flight tests. Fig. 4.1 illustrates the evolution of the control surface position when a 60°/s dynamic runaway is artificially introduced at t=600s.

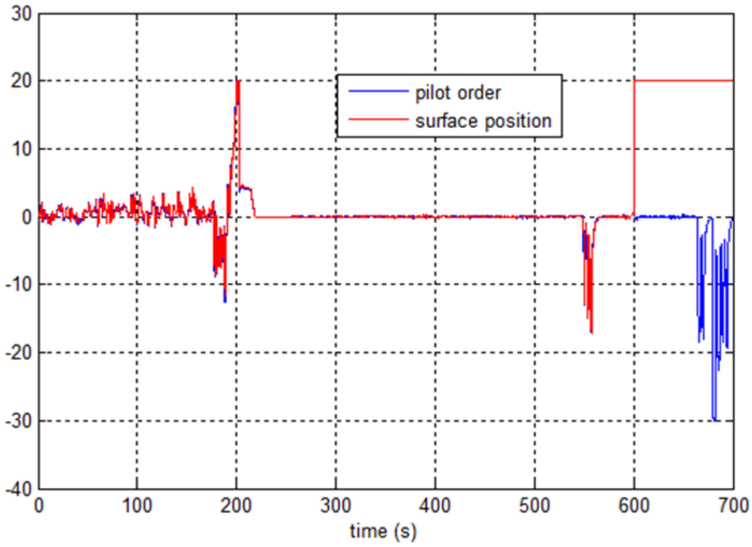

Figure 4.1 : Pilot order and control surface position for runaway case

Fig. 4.2 shows the behavior of the on-line estimated parameter via a modified exponential forgetting algorithm, with an appropriate forgetting factor. As already mentioned, the parameter is sensitive to an abnormal aircraft control surface position. It converges towards zero when a fault occurs.

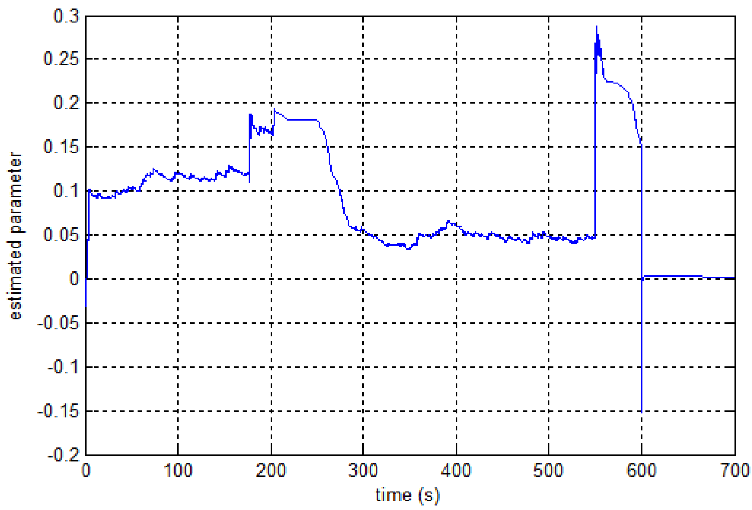

Figure 4.2 : On-line parameter estimate for runaway case

For the CR2 failure detection procedure, a nominal estimate and covariance matrix are set. The covariance matrix characterizes the confidence region about the reference estimate. As it can be seen from Fig. 4.3, the method indicates the runaway after a very short delay. It can be noted that when the inequality described in step a) does not hold, the criterion value is set to zero.

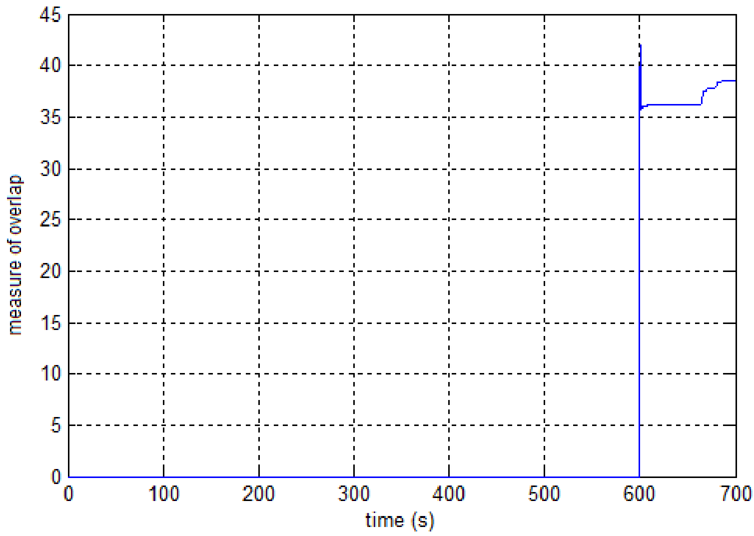

Figure 4.3 : CR2 overlap test for runaway case

For jamming case, simulation results confirm that the proposed method allows control surface jamming detection at small amplitudes and even jamming detection around 0. An example of real elevator position artificially stuck around 0° is given in Fig. 4.4.

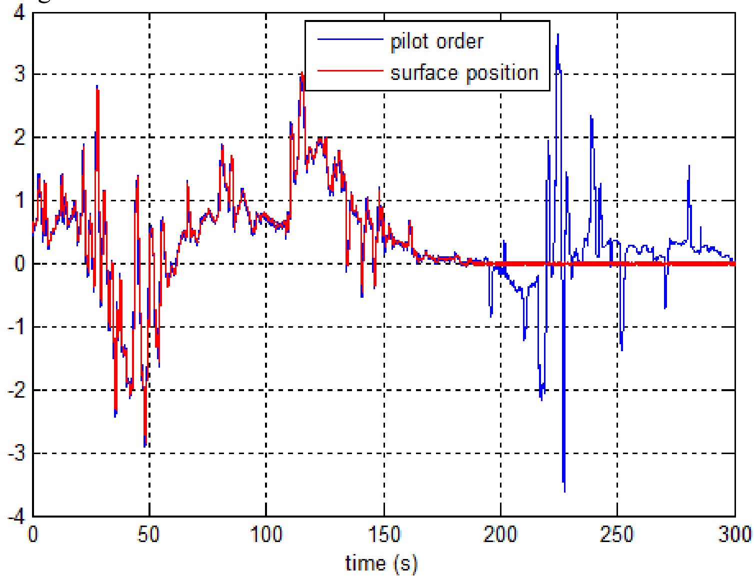

Figure 4.4 : Pilot order and control surface position for jamming case

Figure 4.5 suggests that the estimated parameter is sensitive to control surface jamming case. According to the theoretical section, b_1 converges towards zero when a jamming occurs. The abrupt change of the estimated parameter behaviour is detected by the CR2 decision test. Control surface stuck around 0 is then detected by the new strategy, without degrading the robustness.

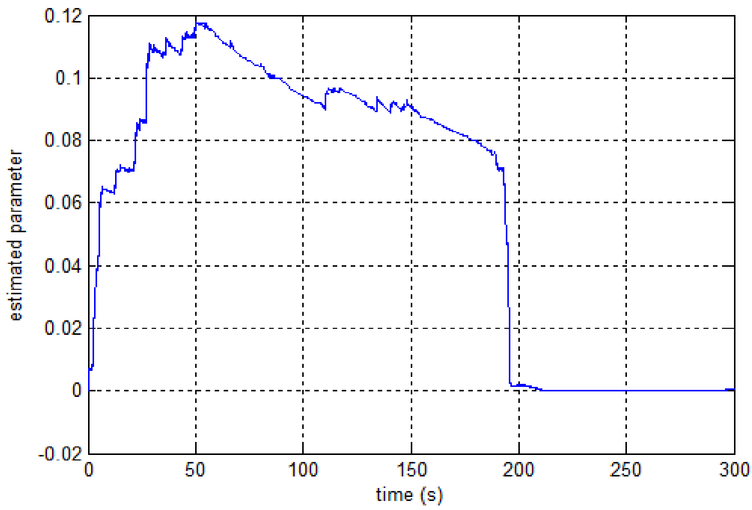

Figure 4.5 : On-line parameter estimate for jamming case

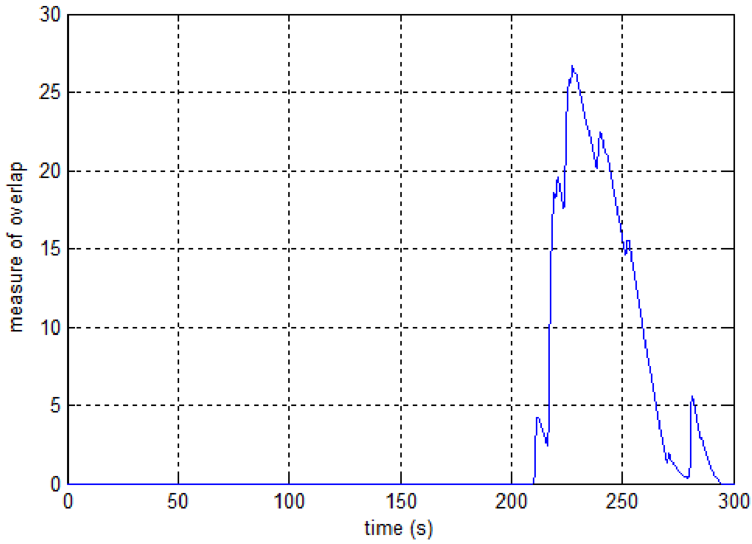

Figure 4.6 : CR2 overlap test for jamming case

5 Concluding remarks

In this paper, a method for fast and robust detection of abnormal control surface position is presented. The detection procedure is based on estimated parametric models followed by a decision test on a carefully chosen direction in the parametric space. That means that some parameters deviations are caused by the occurrence of the researched faults. Firstly, an RLS algorithm with exponential forgetting is used for estimation of a black box model of the control surface servo-loop. The basic algorithm is modified for proper on-line implementation in the FCC, i.e. to prevent covariance wind-up and numerical instability. The directional forgetting is then chosen, where a U-D decomposition of the covariance matrix is used. Secondly, a decision test in the parametric space is applied for fast fault detection. The test checks the agreement of two estimates, one based on on-line estimation via an updated exponential forgetting algorithm and another based on *a priori* information. The technique offers the advantage of low computational load for on-line implementation and a fast response to runaway and jamming cases. Furthermore, the approach is easy to set up and does not require many detailed information about the system to be modeled. Another advantage is the possibility to reuse the method for a new system, i.e. for different actuator models, different moving surfaces or different aircraft families.

References

[1] Gheorghe A, Zolghadri A, Cieslak J, Henry D, Goupil P, Dayre R, Le-Berre H (2011) Early detection of aircraft control surface faults by dedicated Kalman filtering: runaways and jammings. Advanced Control and Diagnosis (ACD), Budapest.

[2] Goupil P, Zolghadri A, Gheorghe A, Cieslak J, Dayre R, Le-Berre H (2012) Airbus efforts towards advanced fault diagnosis for flight control system actuators. R3ASC Conference, Toulouse.

[3] Zolghadri A (1996) An algorithm for real-time failure detection in Kalman filters. IEEE Transactions on Automatic Control 41 (10), 1537-1540.

[4] Zolghadri A (1996) Model based fault detection in a multivariable hydraulic process. 13th IFAC World Congress 253-258, San Francisco, USA.

[5] Zolghadri A, Gheorghe A, Cieslak J, Henry D, Goupil P, Dayre R, Le-Berre H (2011) A model-based solution to robust and early detection of control surface runaways. SAE International Journal of Aerospace 4 (2), 1500-1505.

[6] Ljung L (1998) System Identification: Theory for the User (2nd Edition), Englewood Cliffs NJ: Prentice-Hall.

[7] Bierman GJ (1977) Factorization methods for discrete sequential estimation, Academic Press, New York.

[8] Caglayan AK, Rahnamai K, Allen SM (1988) Detection, Identification and Estimation of Surface Damage/Actuator Failure for High Performance Aircraft. American Control Conference, 2206 – 2212.

[9] Goupil P (2011a) AIRBUS State of the Art and Practices on FDI and FTC in Flight Control System. Control Engineering Practice 19, pp. 524-539. doi: 10.1016/j.conengprac.2010.12.009
[10] Yoshida H, Kumar S, Morita Y (2001) Online fault detection and diagnosis in VAV air handling unit by RARX modeling. Energy and Buildings 33, 391-401.
[11] Minh VT, Ibrahim IB (2010) RARX Estimator and Gain Scheduling Controller for On-Line Fault Detection Controller. International Journal of Automation Technology 4 (1).
[12] Chi-Man Yiu J, Wang S (2007) Multiple ARMAX modeling scheme for forecasting air conditioning system performance. Energy Conversion and Management 48, 2276–2285.
[13] Minh VT (2011) Error and Data Analysis with Recursive Autoregressive Exogenous Estimator. Proc. of 40th Measurement Science Conference MSC, L.A, USA.
[14] Kulhavy R, Karny M (1984) Tracking of Slowly Varying Parameters by Directional Forgetting. In Preprints 9th IFAC World Congress 178-183, Budapest.
[15] Brumback BD, Srinath MD (1987) A chi-square test for fault detection in Kalman filters. IEEE Transactions on Automatic Control 32 (6), 552-554.
[16] Spitzer CR (2001) The Avionics Handbook. Ed. R.C. Dorf. The Electrical Engineering Handbook Series, CRC Press, Boca Raton, London, New York.
[17] FAR/CS 25 Airworthiness standards: Transport category airplane, published by FAA, title 14, part 25, and Certification Specifications for Large Aeroplanes, published by EASA, CS-25.